Estuarine, Coastal and Shelf Science 232 (2020) 106512

Contents lists available at ScienceDirect

Estuarine, Coastal and Shelf Science

journal homepage: http://www.elsevier.com/locate/ecss

Effect of tidal flooding on ecosystem CO_2 and CH_4 fluxes in a salt marsh in the Yellow River Delta

Siyu Wei [a,b], Guangxuan Han [a,*], Xiaojing Chu [a], Weimin Song [a], Wenjun He [a,b], Jianyang Xia [c], Haitao Wu [d]

[a] Key Laboratory of Coastal Zone Environmental Processes and Ecological Remediation, Yantai Institute of Coastal Zone Research, Chinese Academy of Sciences, Yantai, Shandong, 264003, China
[b] University of Chinese Academy of Sciences, Beijing, 100049, China
[c] School of Ecological and Environmental Sciences, East China Normal University, Shanghai, 200241, China
[d] Northeast Institute of Geography and Agroecology, Chinese Academy of Sciences, Changchun, 130102, China

ARTICLE INFO

Keywords:
CO_2
CH_4
Tidal stage
Water level
Soil salinity
Salt marsh

ABSTRACT

Tidal flooding is the basic hydrological feature of a salt marsh, and controls its ecosystem carbon exchange. However, the response of ecosystem carbon exchange to different stages of tidal flooding remains poorly documented. To further explore this issue, we conducted a field experiment to assess the effect of tidal stages (before flooding stage, rising tide stage, tidal flooding stage and after ebbing stage), water levels (a control, a low water level (LWL), a middle water level (MWL) and a high water level (HWL)) and soil salinity on ecosystem CO_2 and CH_4 fluxes in a salt marsh in the Yellow River Delta. Our results showed that the rising tide stage significantly inhibited the uptake of CO_2 (LWL: 1.49 ± 0.23 μmol m^{-2} s^{-1}; MWL: 1.10 ± 0.35 μmol m^{-2} s^{-1}; HWL: 0.54 ± 0.08 μmol m^{-2} s^{-1}). Meanwhile, the rising tide stage also promoted CH_4 emissions of MWL and HWL treatments (MWL: 0.97 ± 0.36 nmol m^{-2} s^{-1}; HWL: 0.93 ± 0.24 nmol m^{-2} s^{-1}). CH_4 emissions of the after ebbing stage was higher than that of the before flooding stage, and this difference was significant of LWL and MWL treatments (LWL: 0.56 ± 0.12 vs 0.38 ± 0.09 nmol m^{-2} s^{-1}; MWL: 0.79 ± 0.13 vs 0.40 ± 0.09 nmol m^{-2} s^{-1}). Moreover, ecosystem CO_2 exchange of the HWL treatment was almost completely suppressed during tidal inundation period. During tidal inundation period, net ecosystem CO_2 exchange (NEE) was significantly positively correlated with water levels, but CH_4 emissions was not significantly affected by water levels. In addition, the rate of CO_2 uptake decreased linearly with soil salinity during the non-inundation period. Therefore, it is necessary to analyze the carbon exchange process coupling with the complete tidal flooding process in future researches.

1. Introduction

Salt marshes have been termed "blue carbon sink" due to its high net primary productivity, high carbon sequestration rates and relatively low CH_4 emissions (Chmura et al., 2003; Kathilankal et al., 2008; Meng et al., 2019). Salt marshes can bury 60.4 Tg of organic carbon per year with a total area of 0.4 × 10^{12} m^2 and an organic carbon burial rate of 151.0 g C m^{-2} y^{-1} (Duarte et al., 2005). Different from other wetland types, salt marshes are subject to periodic tidal flooding. A large amount of SO_4^{2-} carried by tidal flooding inhibits the production of CH_4 in salt marshes (Choi and Wang, 2004). Meanwhile, the anaerobic environment created by tidal flooding inhibits the organic carbon mineralization rates, which is conducive to carbon sequestration of salt marshes (Witte and Giani, 2016; Luo et al., 2019). Therefore, tidal flooding is crucial for maintaining salt marshes as the "blue carbon sink". Furthermore, the tidal flooding process consists of several stages. With the alternation of different tidal stages, the soil and plant will be frequent submerged in tidal water and exposed to the atmosphere (Tong et al., 2014; Yang et al., 2018). These tidal stages include the before flooding stage, the rising tide stage, the tidal flooding stage and the after ebbing stage. Moreover, tidal flooding process also causes changes in many environmental factors, especially water levels and soil characteristics including soil salinity, which further affects the carbon exchange process of a salt marsh (Armstrong et al., 1985; Yamamoto et al.,

* Corresponding author.
E-mail address: gxhan@yic.ac.cn (G. Han).

https://doi.org/10.1016/j.ecss.2019.106512
Received 15 May 2019; Received in revised form 18 November 2019; Accepted 29 November 2019
Available online 5 December 2019

2009; Chmura et al., 2011; Chambers et al., 2013). This effect will also be reflected in the variations of greenhouse gas fluxes dominated by CO_2 and CH_4. Hence, as the basic hydrological feature of a salt marsh, tidal flooding may be the control factor of carbon exchange process. However, the key mechanism of the carbon cycle of salt marshes under tidal flooding effect is still unclear, which will further limit our understanding of the "blue carbon sink" mechanism of salt marshes (Han, 2017).

Among the environmental factors of a salt marsh, soil salinity and water levels are especially important for the ecosystem CO_2 and CH_4 fluxes (Hirota et al., 2007; Poffenbarger et al., 2011; Hu et al., 2017; Li et al., 2018). Soil salinity had an important effect on ecosystem processes, especially of ecosystem CO_2 and CH_4 fluxes (Hu et al., 2017). High salinity tends to inhibit photosynthesis and productivity by influencing the leaf chlorophyll content, protein synthesis, and lipid metabolism of marsh plants (Abdul-Aziz et al., 2018). Similarly, ecosystem respiration (Reco) closely coupled with plant activity will be also reduced with increasing salinity (Neubauer, 2013). The increase of soil salinity can inhibit the activity of microbial cells by osmotic stress. Thus, the emission of CH_4 is negatively correlated with soil salinity of a salt marsh (Olsson et al., 2015; Jr et al., 2016; Yang et al., 2019). Salinity primarily controls CH_4 emissions through two biogeochemical forces. These two forces include the sulfate reduction effect (caused by tidal water) and the ionic effect (Chambers et al., 2013; Hu et al., 2017). In general, the effect of soil salinity on ecosystem CO_2 and CH_4 fluxes is directly reflected in the impact on microbiological processes (Doroski et al., 2019). Moreover, after the tide recedes, the soil that has experienced tidal flooding changed from an oxidizing environment to a reducing environment compared to that of before flooding. Therefore, a better anaerobic environment after the ebb tide will promote CH_4 emissions (Kelley et al., 1995). This phenomenon also indicates that in addition to soil salinity, changes in the redox environment will have an important impact on CH_4 during tidal flooding process (Ford et al., 2012).

During the tidal inundation period, water levels will replace soil salinity as a control factor of ecosystem CO_2 and CH_4 fluxes. Tidal flooding can flush toxic metabolites, relieve plant drought stress and salt stress, thereby promoting absorption of CO_2. However, a higher water level result in a reduction in the effective photosynthetic area and the rate of gas diffusion, which will further inhibit photosynthesis (Han et al., 2015). Moreover, a higher water level can inhibit autotrophic respiration by inducing plant stomatal closure and inhibit heterotrophic respiration by reducing the availability of oxygen in the soil (Chivers et al., 2009; Yang et al., 2018). Different water levels also influence oxidation-reduction status of soil, which affects various metabolisms in carbon cycle (Hirota et al., 2007). Ecosystem CH_4 exchange of a salt marsh could be more sensitive to this change. There is a threshold for water levels control CH_4 emissions, beyond which CH_4 will be discharged in large quantities (Christensen et al., 2003). A suitable water level provides an anaerobic environment while not excessively inundate stems and leaves will promote CH_4 emissions (Van der Nat and Middelburg, 2000).

Coastal wetlands including salt marshes have long been considered vulnerable to sea level rise (McLeod et al., 2011; Kirwan and Megonigal, 2013; Forbrich and Giblin, 2015). Sea level rise will directly cause significant changes in tidal range and the frequency of tidal flooding (Hagen et al., 2013; Abdul-Aziz et al., 2018), which will further threaten the carbon sink strength of a salt marsh (Jones et al., 2018). The Yellow River Delta is one of the most active regions of land-ocean interaction (Han et al., 2018), and its tidal flooding process is affected by sea level rise and sediment movement of the Yellow River.

Unfortunately, the current knowledge of the response of carbon exchange to different tidal stage remains limited, which restricts the understanding of the carbon cycle process of a salt marsh under the background of sea level rise. In this paper, we focus on the effect of tidal flooding on ecosystem CO_2 and CH_4 fluxes. We expected that the variations of ecosystem CO_2 and CH_4 fluxes to different tidal stages is mainly caused by changes in soil salinity, water levels and redox environment. We further hypothesized that: (1) ecosystem CO_2 and CH_4 fluxes during inundation period will be completely inhibited under high water level treatment; (2) the anaerobic environment will significantly promote CH_4 emissions at the after ebbing stage; (3) the higher soil salinity will significantly reduce CO_2 uptake and CH_4 emissions. Based on a field experiment with manipulated tidal stages and water levels, our objectives are (1) to illustrate how the ecosystem CO_2 and CH_4 fluxes response to different tidal stages and (2) to investigate the influences of water levels and soil salinity on ecosystem CO_2 and CH_4 fluxes.

2. Materials and methods

2.1. Study site

This study was conducted in the intertidal zone observation site of the Research Station of Coastal Wetland in the Yellow River Delta, Chinese Academy of Sciences (37°36′56″N, 118°57′51″E). The tidal salt marsh of the Yellow River Delta is one of the typical types of salt marshes in northern China. The terrain is flat and the species composition is very simple, which is dominated by *Suaeda salsa* (Huang et al., 2012). The area belongs to the temperate semi-humid continental monsoon climate, with a moderate-temperature, sufficient sunshine and distinct seasons. The annual average temperature is 12.9 °C, with average annual precipitation of 560 mm (Han et al., 2018). The soil type is coastal tidal saline soil and the soil texture is sandy clay loam. The tide in this area belongs to irregular semidiurnal tide with a mean tidal range of 0.73–1.77 m. The mean seawater salinity was 28 ± 0.42 ppt (Xie et al., 2019). The dissoluble salt content in surface layer of salt soil is very high (>8 g/kg), and its grain composition is dominated by sand and silt (Song et al., 2016).

2.2. Experimental design

We used cylindrical transparent plexiglass chambers (outer diameter was 21 cm, thickness was 0.5 cm and height was 50 cm) as our "plot". Prior to measurement, we installed all plexiglass chambers in preselected locations. The principle of our choice was to keep the number and height of plants in each chamber as consistent as possible. At the end of every experiment, we removed all chambers until the next experiment.

To explore the effects of different water levels during tidal flooding, we designed four experimental treatments in our field experiment: (1) control (no water addition), (2) low water level (1–2 cm, only a small part of the stem of the plant was submerged, LWL), (3) middle water level (5–13 cm, submerged half of the plant, MWL), and (4) high water level (13–24 cm, completely submerged the plant, HWL). Each treatment included 3 replicates. Therefore, the water level of MWL and HWL treatment will vary with the growth of the plant throughout the experimental period. Moreover, total of 5 rounds of measurements were taken for each experiment, and the specific measurement rounds were divided into: before flooding stage, rising tide stage, tidal flooding-3 h stage, tidal flooding-22 h stage and after ebbing-2 h stage. In addition, we simulated the entire tidal flooding process by artificially adding water into chambers or draining water out off chambers.

2.3. Measurements of ecosystem CO_2 and CH_4 fluxes and environmental factors

Ecosystem CO_2 and CH_4 fluxes were measured every two weeks and lasted for the entire growing season of 2018. Measurements were performed using a static cylindrical transparent chamber connected to a LGR Ultraportable Greenhouse Gas Analyzer (UGGA, Los Gatos Research Inc., San Jose, USA) that measures gas concentrations continuously and automatically. In order to prevent the gas in the chamberfrom forming a concentration gradient, a small fan was installed to mix the gas.

Following the measurement of net ecosystem CO_2 exchange (NEE), the chamber would be covered with an opaque cloth to measure ecosystem respiration (Reco). Hence, ecosystem gross primary production (GPP) could be calculated as the difference between NEE and Reco. In addition to the measurement of ecosystem CO_2 and CH_4 fluxes, we also used a 2265FS direct soil EC meter (Spectrum Technologies Inc., Phoenix, AZ, USA) to determine soil salinity (5 cm depth, characterized by soil conductivity in this paper) during the non-inundation stage (Tam and Wong, 1998). During the experiment we also recorded water levels in each chamber.

2.4. Data analysis and statistics

Repeated measures ANOVA was used to examine the difference of ecosystem CO_2 and CH_4 fluxes at different tidal stages and different water levels. In addition, linear regression analysis was used to analyze the relationship between ecosystem CO_2 and CH_4 fluxes and environmental factors (water level and soil salinity). In all tests, a significance level of $P = 0.05$ was used. All statistical analyses were performed under SPSS 13.0 (SPSS for Windows, Chicago, IL, USA) and all graphs were made by Origin 8.0 (OriginLab Inc., Northampton, Massachusetts, USA).

3. Results

3.1. Variations of ecosystem CO_2 and CH_4 fluxes at different tidal stages

3.1.1. Variations of ecosystem CO_2 fluxes at different tidal stages

There was no significant difference in GPP and NEE of the control treatment (Fig. 1). Furthermore, there were few differences in Reco of control treatment, although the rising tide stage and the after ebbing-2 h stage had a higher rate of Reco relative to the other tidal stage. Reco of LWL treatment varied by tidal stages was relatively small (Fig. B). At the rising tide stage, however, both GPP (reduced to 3.46 ± 0.40 μmol m^{-2} s^{-1}) and NEE (increased to -1.49 ± 0.23 μmol m^{-2} s^{-1}) were significantly different from other tidal stages, indicating that the rising tide process significantly inhibited the absorption of CO_2. This phenomenon also had the same performance in the MWL treatment and HWL treatment (Fig. 1C and D). In addition, after 22 h of tidal flooding, NEE of LWL treatment returned to a level similar to that of the before flooding stage (Fig. 1B).

The change of ecosystem CO_2 exchange under the treatment of MWL was relatively complicated (Fig. 1C). At the tidal flooding-3 h stage, Reco increased to 2.10 ± 0.25 μmol m^{-2} s^{-1}, which was the maximum value of the entire tidal flooding process. During the tidal inundation period, the ability to uptake CO_2 of the plant became stronger. The rate of CO_2 uptake reached a maximum after 22 h of flooding (GPP: 4.54 ± 0.52 μmol m^{-2} s^{-1}; NEE: 2.54 ± 0.42 μmol m^{-2} s^{-1}). Moreover, after 2 h of the ebbing tide, the absorption of CO_2 was significantly weaker than that before flooding ($P < 0.01$). Furthermore, in treatments of LWL and HWL, the rate of CO_2 uptake at the after ebbing-2 h stage was also weaker than that of the before flooding stage.

In the HWL treatment, the ecosystem CO_2 exchange was almost completely suppressed due to the complete submerge of the plant during the tidal inundation period, and GPP, Reco and NEE were all close to 0 (Fig. 1D). After the tide receded, both GPP and NEE returned to a level similar to those before flooding, but Reco of the after ebbing stage was significantly higher than before flooding ($P < 0.05$).

3.1.2. Variations of ecosystem CH_4 fluxes at different tidal stages

During the entire experiment, the variations of ecosystem CH_4 fluxes of the control treatment was slightly (Fig. 2A). In the LWL treatment, CH_4 emissions was reduced to 0.31 ± 0.06 nmol m^{-2} s^{-1} at the rising tide stage (Fig. 2B), which was also the minimum of CH_4 emissions throughout the tidal flooding process. After the rising tide, CH_4

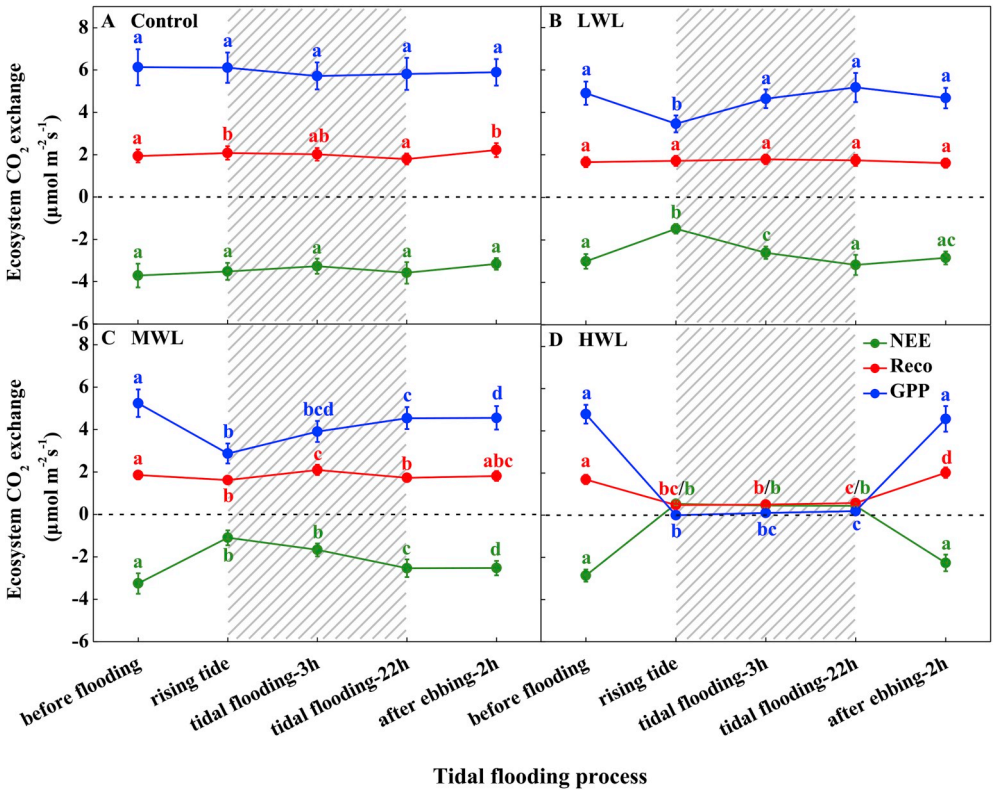

Fig. 1. Variations of mean ecosystem CO_2 fluxes at five different tidal stages. The shaded portion in the figure indicates the period of tidal water inundation. Different lowercase letters in the same line indicate a significant difference of CO_2 fluxes between different tidal stages ($p < 0.05$). Data is presented as mean ± SE. LWL: low water level; MWL: middle water level; HWL: high water level.

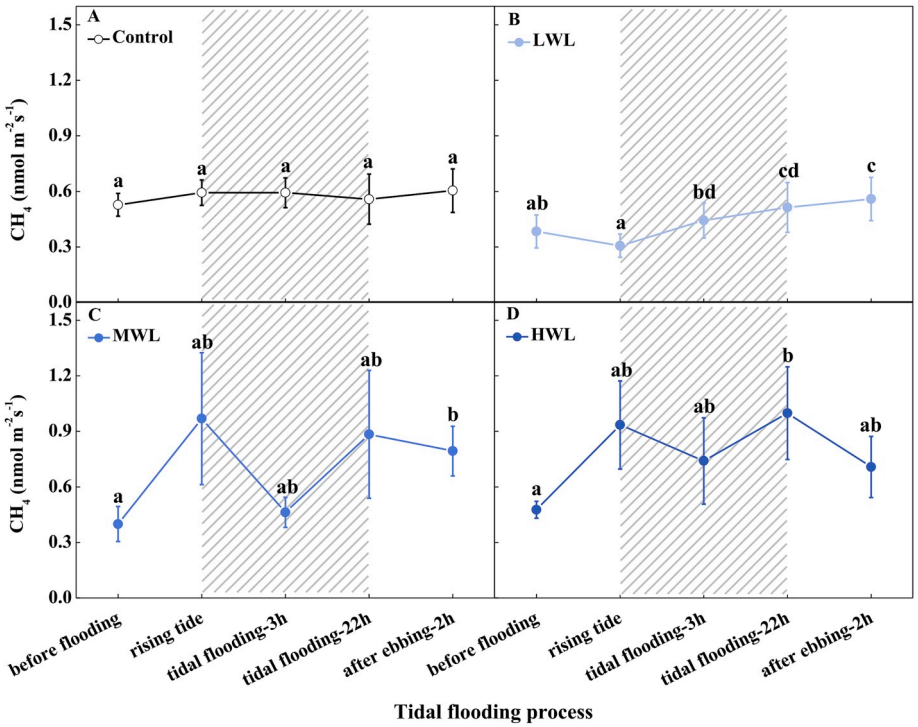

Fig. 2. Variations of mean ecosystem CH_4 fluxes at five different tidal stages. The shaded portion in the figure indicates the period of tidal water inundation. Different lowercase letters indicate a significant difference between different tidal stages ($p < 0.05$). Data is presented as mean ± SE.

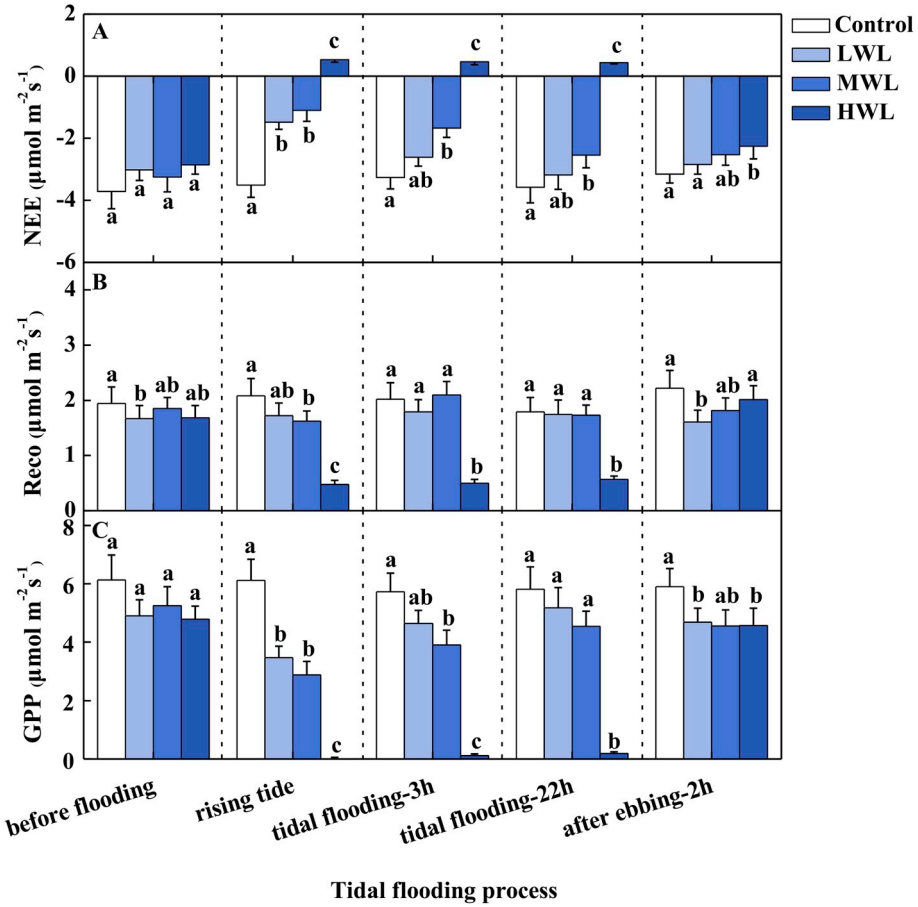

Fig. 3. Variations of mean ecosystem CO_2 fluxes for four water-level treatments. Different lowercase letters under the same tidal stage indicate a significant difference ($p < 0.05$). Data is presented as mean ± SE.

emissions had been rising and reached a maximum of 0.56 ± 0.17 nmol m^{-2} s^{-1} after 2 h after ebbing, which was significantly higher than that of the before flooding stage ($P < 0.05$).

The overall trend of CH_4 emissions in the MWL and HWL was similar (Fig. 2C and D). At the rising tide stage, CH_4 emissions from both treatments increased, but the difference was not significant. In addition, CH_4 emissions after 3 h of tidal flooding were the minimum (MWL: 0.46 ± 0.08 nmol m^{-2} s^{-1}; HWL: 0.74 ± 0.23 nmol m^{-2} s^{-1}) during the tidal inundation period. However, for the MWL treatment, CH_4 emissions at 2 h after the ebb tide was significantly higher than those before flooding ($P < 0.05$), and this difference was not significant in the HWL treatment. In the HWL treatment, the CH_4 emissions of the tidal flooding-22 h stage was the highest relative to other tidal stages.

3.2. Variations of ecosystem CO_2 and CH_4 fluxes with different water levels

3.2.1. Variations of ecosystem CO_2 fluxes with different water levels

There was no significant difference in NEE and GPP between the treatments at the before flooding stage (Fig. 3). At the rising tide stage, NEE of LWL, MWL and HWL treatments were significantly higher than that of the control treatment (similarly, GPP was significantly lower than the GPP of control treatment). Furthermore, during the entire tidal inundation period after the rising tide, ecosystem CO_2 exchange of HWL treatment were significantly suppressed because the plants were completely submerged. The three treatments that were not completely submerged had slight differences in Reco during the tidal inundation period. At the after ebbing-2 h stage, Reco of LWL treatment was the lowest of the four treatments (1.61 ± 0.21 μmol m^{-2} s^{-1}), whereas the NEE of HWL treatment became the maximum value (−2.26 ± 0.40 μmol m^{-2} s^{-1}).

3.2.2. Variations of ecosystem CH_4 fluxes with different water levels

No significant difference in ecosystem CH_4 fluxes was found between the four treatments at the before flooding stage (Fig. 4). However, CH_4 emissions of LWL during rising tide was significantly lower than the other three treatments. Moreover, it should be noted that CH_4 emissions of the MWL and HWL increased to 0.97 ± 0.36 and 0.93 ± 0.24 nmol m^{-2} s^{-1} at the rising tide stage, respectively.

After 3 h of tidal flooding, CH_4 emissions of the four treatments returned to a level that was not significantly different. With the extension of the tidal flooding time, CH_4 emissions of HWL treatment reached to 1.00 ± 0.25 nmol m^{-2} s^{-1}, which was significantly higher than the CH_4 emissions of the LWL treatment ($P < 0.05$). Finally, CH_4 emissions of MWL treatment became the maximum compared with other treatments at the after ebbing-2 h stage.

3.3. Effect of water levels on response of ecosystem CO_2 and CH_4 fluxes to tidal flooding

During the tidal inundation period, ecosystem CO_2 exchange, especially NEE and GPP, showed a remarkable correlation with water levels (Fig. 5). NEE was positively correlation with water levels during the whole tidal inundation period (rising tide: $P < 0.05$, $R^2 = 0.92$; tidal flooding-3 h: $P < 0.01$, $R^2 = 0.98$; tidal flooding-22 h: $P < 0.05$, $R^2 = 0.91$). Correlation analysis also showed that the variation of GPP was significantly and negatively related to water levels at the rising tide stage ($P < 0.05$, $R^2 = 0.95$) and the tidal flooding-3 h stage ($P < 0.05$, $R^2 = 0.94$). However, the relationship between Reco and water levels was significantly and negatively correlated at the rising tide stage ($P < 0.05$, $R^2 = 0.92$). In addition, the correlation between the variation of CH_4 and water levels was not significant during the whole tidal inundation period ($P > 0.05$).

3.4. Effect of soil salinity on response of ecosystem CO_2 and CH_4 fluxes to tidal flooding

Soil salinity had an important effect on ecosystem CO_2 and CH_4 fluxes during the non-inundation period (Fig. 6). Due to the high salinity of seawater immersion, soil salinity was generally higher after the tide receded. Correlation analysis showed that there was a significant positively linear correlation between soil salinity and NEE (Fig. 6B, $P < 0.05$, $R^2 = 0.76$). Similarly, we also found that GPP was significantly negatively related to soil salinity (Fig. 6D, $P < 0.05$, $R^2 = 0.70$). However, we did not find a significant correlation in the relationship between CH_4, Reco and soil salinity (Fig. 6A and C).

4. Discussion

4.1. Response of ecosystem CO_2 and CH_4 fluxes to different tidal stages

Our results demonstrate that the higher soil salinity at the after ebbing stage leaded to a lower CO_2 uptake than the before flooding stage (Fig. 6B). The significant negative correlation between soil salinity and CO_2 uptake also had been found in an experiment conducted in a salt marsh (Abdul-Aziz et al., 2018). Higher soil salinity can dehydrate plants through osmotic stress, which will further reduce plant photosynthesis and primary productivity (Heinsch et al., 2004). Moreover,

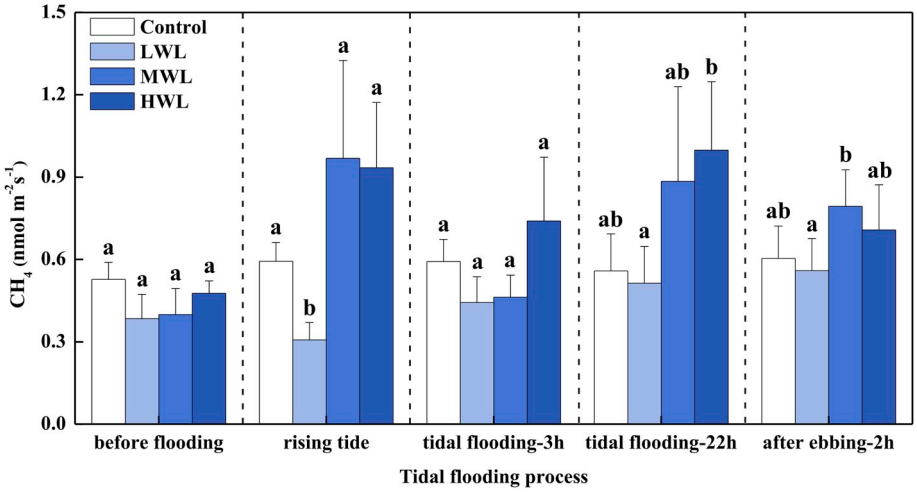

Fig. 4. Variations of mean ecosystem CH_4 fluxes for four water-level treatments. Different lowercase letters under the same tidal stage indicate a significant difference ($p < 0.05$). Data is presented as mean ± SE.

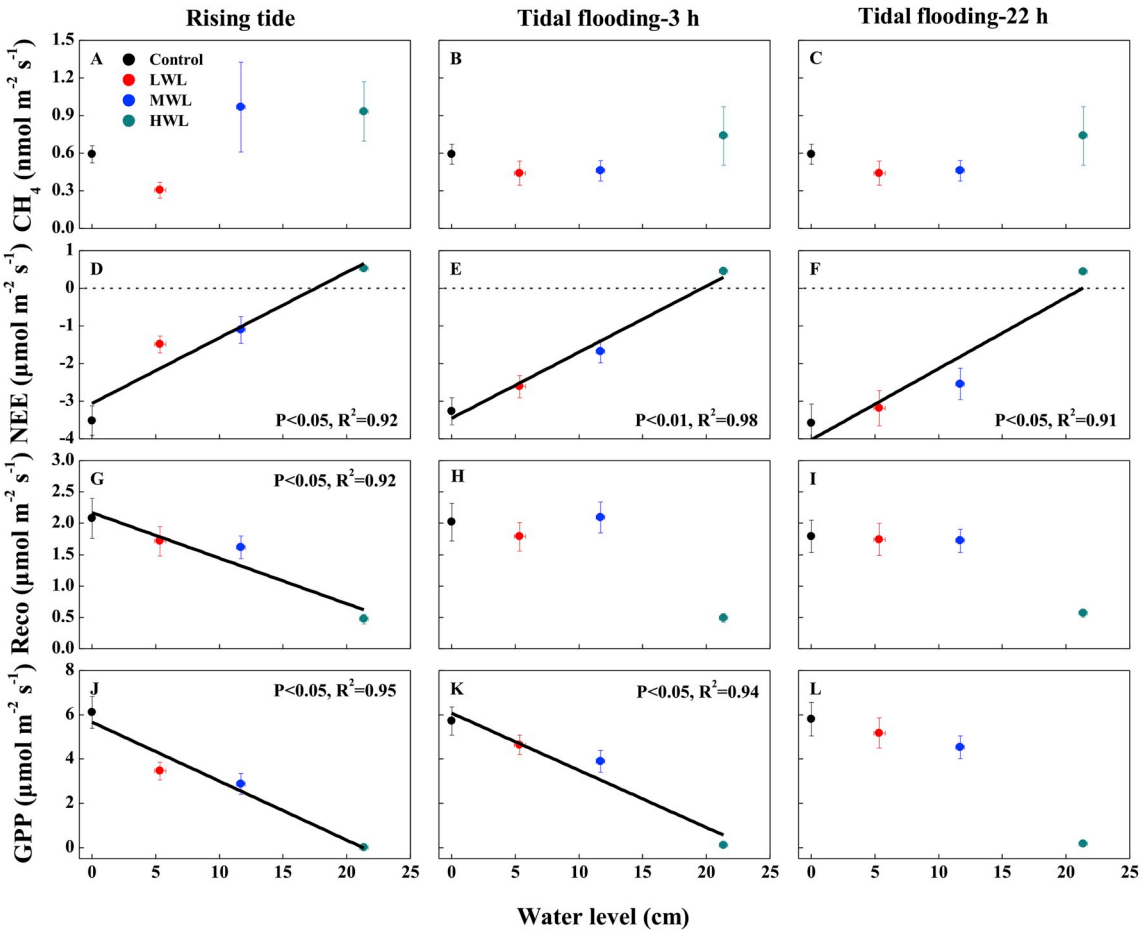

Fig. 5. Linear relationship between water levels and ecosystem CO_2 and CH_4 fluxes during the tidal inundation period. Data is presented as mean ± SE.

anaerobic conditions of the after ebbing stage also affect the photosynthesis of plants. This is because anaerobic conditions result in a switch of aerobic metabolism of plants into less efficient anaerobic fermentation, which will inhibit photosynthesis of plants (Han et al., 2015). Our results also show that the rising tide process significantly suppressed CO_2 uptake. Furthermore, CO_2 uptake of LWL and MWL treatments gradually increased during tidal inundation period. Though it is difficult to explain the inhibitory effect of the rising tide process, physiological response of plant to tidal influx may be related to this phenomenon.

CH_4 emissions of the after ebbing stage was higher than that of the before flooding stage (Fig. 2). The production of CH_4 is an anaerobic process (Deppe et al., 2010). Before the tidal flooding, the anaerobic environment was lacking, which inhibited the production of CH_4 (Chambers et al., 2014). The poor anaerobic environment not only inhibits the production of CH_4, but also promotes the oxidation of CH_4 in the soil oxide layer, thereby reducing CH_4 emissions (Chen et al., 2013). The tidal inundation period has provided a suitable anaerobic environment for the production of CH_4, but CH_4 cannot be released due to the tidal barrier. After the tide recedes, the barrier effect of tidal water disappears, CH_4 that was previously produced by the soil can be released to the atmosphere (Singh et al., 2000; Li et al., 2018).

Changes of soil redox environment caused by tidal flooding can also explain the relationship between CH_4 and soil salinity (Fig. 6A). Although the correlation between CH_4 emissions and soil salinity was not significant, the overall trend was evident: CH_4 emissions were higher under high soil salinity environment at the after ebbing stage. In previous studies, CH_4 fluxes usually decreased with higher soil salinity (Olsson et al., 2015; Jr et al., 2016; Yang et al., 2019), and this relationship was caused by the sulfate reduction effect related to abundant SO_4^{2-} and the ionic effect caused by an increase in the ionic strength (Chambers et al., 2013; Hu et al., 2017). Our seemingly contradictory results demonstrate that in addition to salinity, soil redox environment could be an important factor affecting CH_4 fluxes (Livesley and Andrusiak, 2012). After the tidal water receded, a better anaerobic environment promoted the production of CH_4. In addition, the increased salinity could have led to a decrease in humic substances through salt-induced flocculation of dissolved organic matter. Humic substances can reduce CH_4 production through thermodynamically favorable organic electron acceptors (Ardon et al., 2018). Therefore, the effect of reduced humic substances caused by high salinity is also one of the reasons for promoting CH_4 emissions.

4.2. *Response of ecosystem CO_2 and CH_4 fluxes to water levels during the tidal inundation period*

During the tidal inundation period, the uptake rate of CO_2 was decreased with the increase of water level (Fig. 5). This relationship can be explained by (1) higher water levels will submerge more leaves, reducing more effective photosynthetic leaf area, and (2) higher water levels will reduce photosynthesis by limiting light and CO_2 diffusion in the tidal water (Colmer et al., 2011; Jimenez et al., 2012). However, the relationship between CO_2 uptake and water levels often varies with experimental condition. Researchers have found that elevated water levels significantly enhance CO_2 uptake in temperate cutover fens (Minke et al., 2016). In addition, in an experiment conducted in the Yellow River Delta, the relationship between CO_2 uptake and water levels was varied with different locations (Chen et al., 2018).

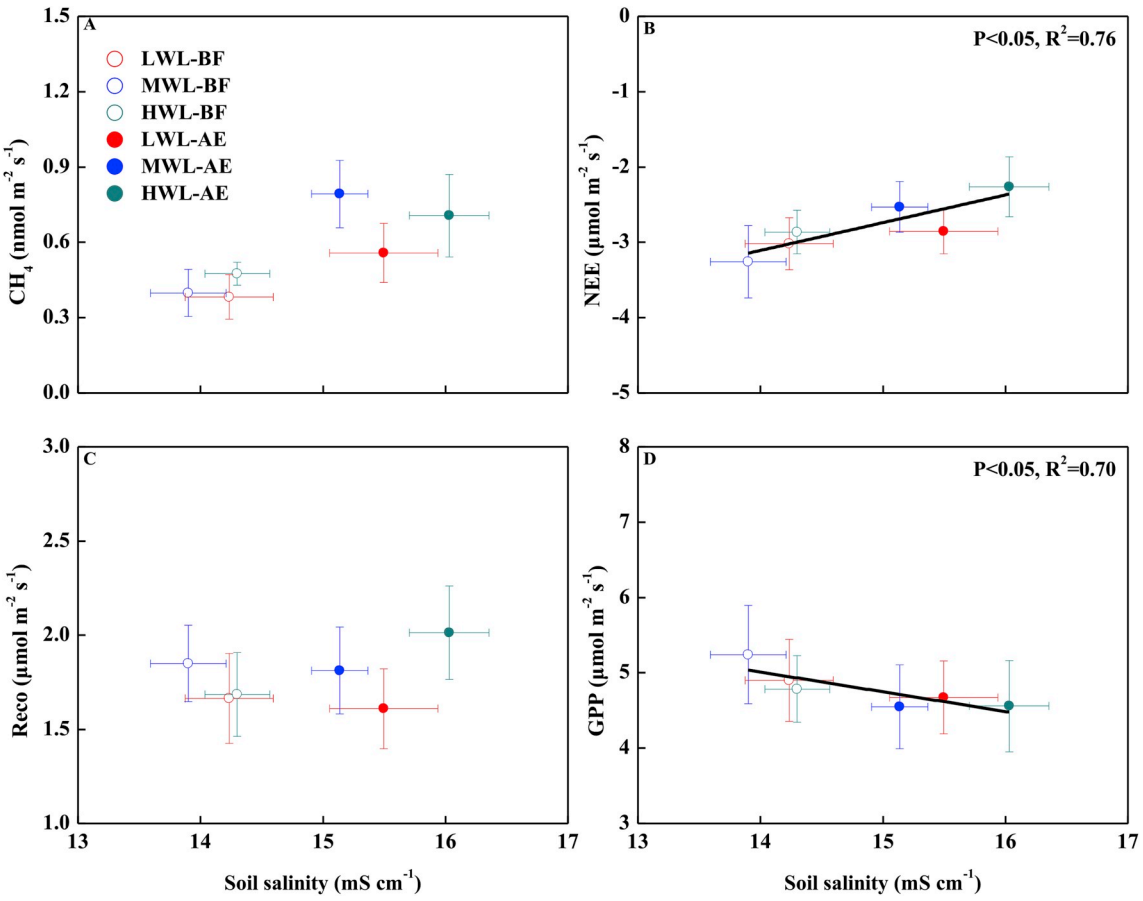

Fig. 6. Linear relationship between soil salinity and ecosystem CO_2 and CH_4 fluxes during the non-inundation period. The before flooding stage is abbreviated as BF and the after ebbing stage is abbreviated as AE. Data is presented as mean ± SE.

Furthermore, ecosystem CO_2 exchange of HWL treatment during the tidal inundation period was nearly completely suppressed (Fig. 1D). This result of our study is similar to that of Moffett et al. (2010), ecosystem CO_2 exchange was completely suppressed under prolonged tidal inundation (Moffett et al., 2010). During the tidal inundation period, the plant was completely submerged in the HWL treatment. First, all the leaves had been submerged so that photosynthesis was completely suppressed. Second, the tidal water forms a gas diffusion barrier. The barrier effect of tidal water can inhibit CO_2 released from plant respiration and soil respiration. Meanwhile, part of the CO_2 will dissolve in tidal water (Guo et al., 2009). Finally, higher water levels reduces the availability of O_2 in the soil. Therefore, activity of aerobic community and the aerobic respiration of the plant roots will be inhibited (Jimenez et al., 2012).

The effect of water levels on ecosystem CH_4 fluxes had different performances during the tidal flooding process. In the MWL and HWL treatments, which were with higher water levels, the rising tide process had an obviously increase in CH_4 emissions (Fig. 2B and C). The main reason is that the rapid influx of tidal water will cause the pressure of the soil pores to increase. Thereby extruding CH_4 from the soil pores and releasing it into the atmosphere (Yamamoto et al., 2009). However, we did not observe a similar phenomenon in LWL treatment due to the pressure generated by less water was not enough to squeeze out CH_4 from the soil pores.

We also found that in the LWL, MWL and HWL treatments, CH_4 emissions of the tidal flooding-22 h stage was relatively high during the whole tidal flooding process (Fig. 2). In the MWL and HWL treatments, since the higher water level submerged part of the plant, CH_4 emissions was relatively low when the inundation time was short (3 h). As the inundation time prolonged (22 h), the CH_4 produced from soil will slowly enrich in the tidal water and eventually be released into the atmosphere. After 22 h of tidal flooding, the difference in CH_4 emissions between treatments of MWL and HWL with treatments of LWL and control had been significant (Fig. 4). This difference may be mainly attributed to (1) better anaerobic environment formed by higher water levels; (2) flushing of the surface soil and the crab burrowing can enhance the exchange of gaseous compounds between the soil and the tidal water, therefore causing the enrichment of CH_4 in the tidal water and then released into the atmosphere (Jacotot et al., 2018; Call et al., 2019).

5. Conclusions

Our results demonstrated that different tidal stages of the tidal flooding process along with the changes in water levels and soil salinity have a critical impact on ecosystem CO_2 and CH_4 fluxes. Our findings could be summarized as follows:

- CO_2 and CH_4 fluxes fluctuated notably with different tidal stages. Changes in soil salinity and soil redox environment were the main environmental factors controlling CO_2 and CH_4 fluxes at the before flooding stage and the after ebbing stage. Moreover, water level replaced the above two factors to control CO_2 and CH_4 fluxes during tidal inundation period.
- The increasing water levels inhibited the rate of CO_2 uptake. Moreover, ecosystem CO_2 exchange was completely inhibited when tidal water completely submerged the plant.
- Higher soil salinity reduced the rate of CO_2 uptake. In addition, CH_4 fluxes was more sensitive to the changes in soil redox environment,

which was mainly manifested by more CH_4 emissions at the after ebbing stage than the before flooding stage.

In this study, we measured soil salinity during the non-inundation period, and we did not measure any other soil properties. This could be limitations of our study. Hence, further research should examine soil properties and other environmental factors at different tidal stages to clarify the effect of tidal flooding on ecosystem CO_2 and CH_4 fluxes of salt marshes.

Author contribution

Siyu Wei: Conceptualization, Formal analysis, Investigation, Data Curation, Visualization, Writing - Original Draft.

Guangxuan Han*: Supervision, Conceptualization, Writing - Review & Editing; Project administration.

Xiaojing Chu: Formal analysis, Data Curation, Writing - Original Draft.

Weimin Song: Investigation, Resources.

Wenjun He: Investigation, Visualization.

Jianyang Xia: Writing - Review & Editing, Project administration.

Haitao Wu: Writing - Review & Editing, Project administration.

Declaration of competing interest

The authors declare that they have no known competing financial interests or personal relationships that could have appeared to influence the work reported in this paper.

Acknowledgements

This research was funded by the Strategic Priority Research Program of the Chinese Academy of Sciences, China (XDA23050202) and the National Natural Science Foundation of China (41671089). We are grateful for the support from Yellow River Delta Ecological Research Station of Coastal Wetland, CAS, and also thank two anonymous reviewers for their expert advice and fruitful comments.

References

Abdul-Aziz, O.I., Ishtiaq, K.S., Tang, J.W., Moseman-Valtierra, S., Kroeger, K.D., Gonneea, M.E., Mora, J., Morkeski, K., 2018. Environmental controls, emergent scaling, and predictions of greenhouse gas (GHG) fluxes in coastal salt marshes. J. Geophys. Res.-Biogeosci. 123 (7), 2234–2256.

Ardon, M., Helton, A.M., Bernhardt, E.S., 2018. Salinity effects on greenhouse gas emissions from wetland soils are contingent upon hydrologic setting: a microcosm experiment. Biogeochemistry 140 (2), 217–232.

Armstrong, W., Wright, E.J., Lythe, S., Gaynard, T.J., 1985. Plant zonation and the effects of the spring-neap tidal cycle on soil aeration in a humber salt marsh. J. Ecol. 73 (1), 323–339.

Call, M., Santos, I.R., Dittmar, T., de Rezende, C.E., Asp, N.E., Maher, D.T., 2019. High pore-water derived CO_2 and CH_4 emissions from a macro-tidal mangrove creek in the Amazon region. Geochem. Cosmochim. Acta 247, 106–120.

Chambers, L.G., Davis, S.E., Troxler, T., Boyer, J.N., Downey-Wall, A., Scinto, L.J., 2014. Biogeochemical effects of simulated sea level rise on carbon loss in an Everglades mangrove peat soil. Hydrobiologia 726 (1), 195–211.

Chambers, L.G., Osborne, T.Z., Reddy, K.R., 2013. Effect of salinity-altering pulsing events on soil organic carbon loss along an intertidal wetland gradient: a laboratory experiment. Biogeochemistry 115 (1–3), 363–383.

Chen, H., Zhu, Q.A., Peng, C.H., Wu, N., Wang, Y.F., Fang, X.Q., Jiang, H., Xiang, W.H., Chang, J., Deng, X.W., Yu, G.R., 2013. Methane emissions from rice paddies natural wetlands, lakes in China: synthesis new estimate. Glob. Chang. Biol. 19 (1), 19–32.

Chen, Q.F., Guo, B.B., Zhao, C.S., Xing, B.X., 2018. Characteristics of CH_4 and CO_2 emissions and influence of water and salinity in the Yellow River delta wetland, China. Environ. Pollut. 239, 289–299.

Chivers, M.R., Turetsky, M.R., Waddington, J.M., Harden, J.W., McGuire, A.D., 2009. Effects of experimental water table and temperature manipulations on ecosystem CO_2 fluxes in an Alaskan rich fen. Ecosystems 12 (8), 1329–1342.

Chmura, G.L., Anisfeld, S.C., Cahoon, D.R., Lynch, J.C., 2003. Global carbon sequestration in tidal, saline wetland soils. Glob. Biogeochem. Cycles 17 (4), 1111.

Chmura, G.L., Kellman, L., Guntenspergen, G.R., 2011. The greenhouse gas flux and potential global warming feedbacks of a northern macrotidal and microtidal salt marsh. Environ. Res. Lett. 6 (4), 044016.

Choi, Y.H., Wang, Y., 2004. Dynamics of carbon sequestration in a coastal wetland using radiocarbon measurements. Glob. Biogeochem. Cycles 18 (4).

Christensen, T.R., Ekberg, A., Ström, L., Mastepanov, M., Panikov, N., Öquist, M., Bo, H. S., Nykänen, H., Martikainen, P.J., Oskarsson, H., 2003. Factors controlling large scale variations in methane emissions from wetlands. Geophys. Res. Lett. 30 (7), 1414–1419.

Colmer, T.D., Winkel, A., Pedersen, O., 2011. A perspective on underwater photosynthesis in submerged terrestrial wetland plants. AoB PLANTS plr030, 2011.

Deppe, M., Knorr, K.H., Mcknight, D.M., Blodau, C., 2010. Effects of short-term drying and irrigation on CO_2 and CH_4 production and emission from mesocosms of a northern bog and an alpine fen. Biogeochemistry 100 (1–3), 89–103.

Doroski, A.A., Helton, A.M., Vadas, T.M., 2019. Greenhouse gas fluxes from coastal wetlands at the intersection of urban pollution and saltwater intrusion: a soil core experiment. Soil Biol. Biochem. 131, 44–53.

Duarte, C.M., Middelburg, J.J., Caraco, N., 2005. Major role of marine vegetation on the oceanic carbon cycle. Biogeosciences 2 (1), 1–8.

Forbrich, I., Giblin, A.E., 2015. Marsh-atmosphere CO_2 exchange in a New England salt marsh. J. Geophys. Res.-Biogeosci. 120 (9), 1825–1838.

Ford, H., Garbutt, A., Jones, L., Jones, D.L., 2012. Methane, carbon dioxide and nitrous oxide fluxes from a temperate salt marsh: grazing management does not alter Global Warming Potential. Estuar. Coast Shelf Sci. 113, 182–191.

Guo, H.Q., Noormets, A., Zhao, B., Chen, J.Q., Sun, G., Gu, Y.J., Li, B., Chen, J.K., 2009. Tidal effects on net ecosystem exchange of carbon in an estuarine wetland. Agric. For. Meteorol. 149 (11), 1820–1828.

Hagen, S.C., Morris, J.T., Bacopoulos, P., Weishampel, J.F., 2013. Sea-level rise impact on a salt marsh system of the lower St. Johns river. J. Waterw. Port, Coast. Ocean Eng. 139 (2), 118–125.

Han, G., 2017. Effect of tidal action and drying-wetting cycles on carbon exchange in a salt marsh: progress and prospects. Acta Ecol. Sin. 37 (24), 8170–8178 (in Chinese).

Han, G.X., Chu, X.J., Xing, Q.H., Li, D.J., Yu, J.B., Luo, Y.Q., Wang, G.M., Mao, P.L., Rafique, R., 2015. Effects of episodic flooding on the net ecosystem CO_2 exchange of a supratidal wetland in the Yellow River Delta. J. Geophys. Res.-Biogeosci. 120 (8), 1506–1520.

Han, G.X., Sun, B.Y., Chu, X.J., Xing, Q.H., Song, W.M., Xia, J.Y., 2018. Precipitation events reduce soil respiration in a coastal wetland based on four-year continuous field measurements. Agric. For. Meteorol. 256–257, 292–303.

Heinsch, F.A., Heilman, J.L., McInnes, K.J., Cobos, D.R., Zuberer, D.A., Roelke, D.L., 2004. Carbon dioxide exchange in a high marsh on the Texas Gulf Coast: effects of freshwater availability. Agric. For. Meteorol. 125 (1–2), 159–172.

Hirota, M., Senga, Y., Seike, Y., Nohara, S., Kunii, H., 2007. Fluxes of carbon dioxide, methane and nitrous oxide in two contrastive fringing zones of coastal lagoon, Lake Nakaumi, Japan. Chemosphere 68 (3), 597–603.

Hu, M.J., Ren, H.X., Ren, P., Li, J.B., Wilson, B.J., Tong, C., 2017. Response of gaseous carbon emissions to low-level salinity increase in tidal marsh ecosystem of the Min River estuary, Southeastern China. J. Environ. Sci. 52 (2), 210–222.

Huang, L., Bai, J., Chen, B., Zhang, K., Huang, C., Liu, P., 2012. Two-decade wetland cultivation and its effects on soil properties in salt marshes in the Yellow River Delta, China. Ecol. Inf. 10, 49–55.

Jacotot, A., Marchand, C., Allenbach, M., 2018. Tidal variability of CO_2 and CH_4 emissions from the water column within a Rhizophora mangrove forest (New Caledonia). Sci. Total Environ. 631–632, 334–340.

Jimenez, K.L., Starr, G., Staudhammer, C.L., Schedlbauer, J.L., Loescher, H.W., Malone, S.L., Oberbauer, S.F., 2012. Carbon dioxide exchange rates from short- and long-hydroperiod Everglades freshwater marsh. J. Geophys. Res.-Biogeosci. 117, G04009.

Jones, S.F., Stagg, C.L., Krauss, K.W., Hester, M.W., 2018. Flooding alters plant-mediated carbon cycling independently of elevated atmospheric CO_2 concentrations. J. Geophys. Res.-Biogeosci. 123 (6), 1976–1987.

Jr, G.O.H., Perez, B.C., Mcwhorter, D.E., Krauss, K.W., Johnson, D.J., Raynie, R.C., Killebrew, C.J., 2016. Ecosystem level methane fluxes from tidal freshwater and brackish marshes of the Mississippi River Delta: implications for coastal wetland carbon projects. Wetlands 36 (3), 401–413.

Kathilankal, J.C., Mozdzer, T.J., Fuentes, J.D., D'Odorico, P., McGlathery, K.J., Zieman, J.C., 2008. Tidal influences on carbon assimilation by a salt marsh. Environ. Res. Lett. 3 (4), 044010.

Kelley, C.A., Martens, C.S., Ussler, W., 1995. Methane dynamics across a tidally flooded riverbank margin. Limnol. Oceanogr. 40 (6), 1112–1129.

Kirwan, M.L., Megonigal, J.P., 2013. Tidal wetland stability in the face of human impacts and sea-level rise. Nature 504 (7478), 53–60.

Li, H., Dai, S.Q., Ouyang, Z.T., Xie, X., Guo, H.Q., Gu, C.H., Xiao, X.M., Ge, Z.M., Peng, C. H., Zhao, B., 2018. Multi-scale temporal variation of methane flux and its controls in a subtropical tidal salt marsh in eastern China. Biogeochemistry 137 (1–2), 163–179.

Livesley, S.J., Andrusiak, S.M., 2012. Temperate mangrove and salt marsh sediments are a small methane and nitrous oxide source but important carbon store. Estuar. Coast Shelf Sci. 97, 19–27.

Luo, M., Huang, J.-F., Zhu, W.-F., Tong, C., 2019. Impacts of increasing salinity and inundation on rates and pathways of organic carbon mineralization in tidal wetlands: a review. Hydrobiologia 827 (1), 31–49.

McLeod, E., Chmura, G.L., Bouillon, S., Salm, R., Bjork, M., Duarte, C.M., Lovelock, C.E., Schlesinger, W.H., Silliman, B.R., 2011. A blueprint for blue carbon: toward an improved understanding of the role of vegetated coastal habitats in sequestering CO_2. Front. Ecol. Environ. 9 (10), 552–560.

Meng, W.Q., Feagin, R.A., Hu, B.B., He, M.X., Li, H.Y., 2019. The spatial distribution of blue carbon in the coastal wetlands of China. Estuar. Coast Shelf Sci. 222, 13–20.

Minke, M., Augustin, J., Burlo, A., Yarmashuk, T., Chuvashova, H., Thiele, A., Freibauer, A., Tikhonov, V., Hoffmann, M., 2016. Water level, vegetation

composition and plant productivity explain greenhouse gas fluxes in temperate cutover fens after inundation. Biogeosciences 13 (13), 3945–3970.
Moffett, K.B., Wolf, A., Berry, J.A., Gorelick, S.M., 2010. Salt marsh-atmosphere exchange of energy, water vapor, and carbon dioxide: effects of tidal flooding and biophysical controls. Water Resour. Res. 46, W10525.
Neubauer, S.C., 2013. Ecosystem responses of a tidal freshwater marsh experiencing saltwater intrusion and altered hydrology. Estuar. Coasts 36 (3), 491–507.
Olsson, L., Ye, S., Yu, X., Wei, M., Krauss, K.W., Brix, H., 2015. Factors influencing CO_2 and CH_4 emissions from coastal wetlands in the Liaohe Delta, Northeast China. Biogeosciences 12 (16), 4965–4977.
Poffenbarger, H.J., Needelman, B.A., Megonigal, J.P., 2011. Salinity influence on methane emissions from tidal marshes. Wetlands 31 (5), 831–842.
Singh, S.N., Kulshreshtha, K., Agnihotri, S., 2000. Seasonal dynamics of methane emission from wetlands. Chemosphere Global Change Sci. 2 (1), 39–46.
Song, H.L., Liu, X.T., Cui, B.S., He, Q., Gu, B.H., Bai, J.H., Liu, X.H., 2016. Anthropogenic effects on fluxes of ecosystem respiration and methane in the Yellow River estuary, China. Wetlands 36 (Suppl. 1), 113–123.
Tam, N.F.Y., Wong, Y.S., 1998. Variations of soil nutrient and organic matter content in a subtropical mangrove ecosystem. Water Air Soil Pollut. 103 (1–4), 245–261.
Tong, C., Wang, C., Huang, J.F., Wang, W.Q., E, Y., Liao, J., Yao, C., 2014. Ecosystem respiration does not differ before and after tidal inundation in brackish marshes of the Min river estuary, southeast China. Wetlands 34 (2), 225–233.
Van der Nat, F.J., Middelburg, J.J., 2000. Methane emission from tidal freshwater marshes. Biogeochemistry 49 (2), 103–121.
Witte, S., Giani, L., 2016. Greenhouse gas emission and balance of marshes at the Southern North sea coast. Wetlands 36 (1), 121–132.
Xie, T., Cui, B., Li, S., Zhang, S., 2019. Management of soil thresholds for seedling emergence to re-establish plant species on bare flats in coastal salt marshes. Hydrobiologia 827 (1), 51–63.
Yamamoto, A., Hirota, M., Suzuki, S., Oe, Y., Zhang, P., Mariko, S., 2009. Effects of tidal fluctuations on CO_2 and CH_4 fluxes in the littoral zone of a brackish-water lake. Limnology 10 (3), 229–237.
Yang, P., Lai, D.Y.F., Huang, J.F., Zhang, L.H., Tong, C., 2018. Temporal variations and temperature sensitivity of ecosystem respiration in three brackish marsh communities in the Min River Estuary, Southeast China. Geoderma 327, 138–150.
Yang, P., Wang, M.H., Lai, D.Y.F., Chun, K.P., Huang, J.F., Wan, S.A., Bastviken, D., Tong, C., 2019. Methane dynamics in an estuarine brackish Cyperus malaccensis marsh: production and porewater concentration in soils, and net emissions to the atmosphere over five years. Geoderma 337, 132–142.